TOWARDS QUANTIFICATION OF THE BRAIN'S SHEET STRUCTURE: EVALUATION OF THE DISCRETE LIE BRACKET

Chantal M.W. Tax[1], Tom C.J. Dela Haije[2], Andrea Fuster[2], Remco Duits[2], Max A. Viergever[1], Luc M.J. Florack[2], and Alexander Leemans[1]
[1]*Image Sciences Institute, University Medical Center Utrecht, Utrecht, Utrecht, Netherlands,* [2]*Imaging Science & Technology, Eindhoven University of Technology, Eindhoven, Noord-Brabant, Netherlands*

Purpose: A three-dimensional Manhattan street grid or the intricate streets of Victorian London, which structure reflects our brain's organization best? This central question added three Science publications to the diffusion MRI (dMRI) literature [1-3]. Wedeen et al. (2012a,b) [1,3] conjectured that cerebral white matter pathways form a three-dimensional grid of interwoven sheets. Catani et al. (2012) [2] concluded that the grid pattern is most likely an artifact, biased by the limitations of the techniques used in Wedeen et al. (2012a). In order to prove or disprove the occurrence of sheet structure, more extensive quantitative analyses are needed. In this work, we aim for a formalization of the terminology, and evaluate the validity of the discrete Lie bracket (estimated as proposed in Wedeen et al. (2012a)) as a tool to quantify the occurrence of sheet structure on simulated vector fields as a function of noise and spatial resolution.

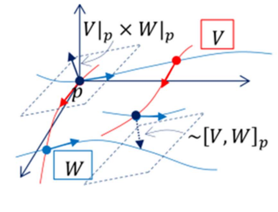

Fig. 1: If the Lie bracket lies in the dashed plane, involutivity is satisfied. To approach Lie bracket: For small time h_1, follow the integral curve of V through p, curve of W during h_2, and subsequently curve of W through p (time h_2), curve of V (time h_1).

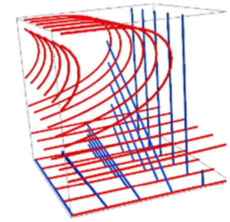

Fig. 2: Vector field pair 2: V and $W$are respectively $(\cos(\pi\tilde{z}^3), 0, \sin(\pi\tilde{z}^3))^T$, $(0, \cos(\pi\tilde{x}^3), \sin(\pi\tilde{x}^3))^T$, with $\tilde{x} = (x-10)/20$ and $\tilde{z} = (z-10)/20$.

Theory: From a set of diffusion or fiber orientation distribution functions (ODFs) on each position of the brain (a manifold $M \subset \mathbb{R}^3$) obtained from any suitable dMRI reconstruction technique, one can obtain a smooth vector field $V: N_V \to \mathbb{R}^3$ (with $N_V \subset M$) derived from ODF maxima. A single vector field can be integrated to obtain a family of streamlines (or integral curves) $s \mapsto \gamma_V(s)$ such that $d\gamma_V(s)/ds = V|_{\gamma_V(s)}$, where s denotes the arc-length parameter. This integration can be extended to two vector fields V and W, resulting in an integral surface S (the *sheet*) whose tangent plane at p is spanned by $V|_p$ and $W|_p$. The requirements for such a surface to exist are formalized in the Frobenius theorem [4]. The Lie bracket of vector fields V and W on $N_V \cap N_W \subset \mathbb{R}^3$ is a bilinear operator defining a third vector field $[V,W] = J_W \cdot V - J_V \cdot W$, with J_X the Jacobian of a vector field X. The Frobenius theorem states that the sheet S exists if and only if $[V,W]$ lies in the plane spanned by V and W (i.e. "*the normal component of the Lie bracket*" [1] $[V,W]_p^{\perp} = [V,W]_p \cdot (V|_p \times W|_p)$ should be zero) for all points $p \in S$ (Fig. 1.).

Methods: Lie bracket calculations: Differential operators on vector fields are notoriously difficult to implement, often requiring considerable implicit smoothing. In Wedeen et al. (2012a) the authors opt instead to move around along the integral curves [6] and consider the difference vectors $D|_p(h_1,h_2) = \gamma_W|_q(h_2) - \gamma_V|_r(h_1)$, where $q = \gamma_V|_p(h_1)$, $r = \gamma_W|_p(h_2)$ and h_1 and h_2 are step sizes, see Fig. 1. This difference vector at p is related to the local Lie bracket according to $D|_p(h_1,h_2) = h_1 h_2 [V,W]_p + \Delta(h_1,h_2)$, with $\Delta(h_1,h_2)$ correction terms of third and higher orders in h_1 and h_2 (i.e. $O((h_1)^2 h_2)$ and similar terms) [5]. While this shows that for small h_1 and h_2 we have the *linear* relationship $D|_p(h_1,h_2)/(h_1 h_2) \approx [V,W]_p$, it should be noted that the correction terms $\Delta(h_1,h_2)$ can be significant. Vector field simulations: Two different pairs of analytical unit vector fields defined on the domain $[-10\,mm, 10\,mm]^3$ were sampled on a Cartesian grid (x,y,z) with constant spacing $\delta\ mm$. Pair 1 consists of vector fields $V_1 = \{1, 0, 0.1x\}^T$, $W_1 = \{0, 1, 0.1y\}^T$, which have a zero Lie bracket by design and are locally tangent to the surface $z(x,y) = 0.05(x^2+y^2)$. For pair 2 no tangent surface exists (Fig. 2). Where indicated, angular deviations θ were added to the vector field sampled from the von Mises distribution with κ analogous to the inverse variance σ^{-2}.

Results: We compare for each of the vector field pairs the Lie bracket estimates $E_p(V,W)$ to the analytically calculated Lie bracket $[V,W]_p$, with p the origin. Analogous to Wedeen et al. (2012a) [1], we determine $E_p(V,W)$ by using the linear relationship between $D|_p(h_1,h_2)$ and $h_1 h_2$ ($\Delta(h_1,h_2)$ assumed to be small): the components $E_p^i(V,W)$ equal the slope of the least squares fit to the scatter plots of $D^i|_p(h_1,h_2)$ versus $|h_1 h_2|$ ($h_1, h_2 \in [-5\,mm, 5\,mm]$), see Fig. 3. The fit is very much dependent on the choice of maximum $|h_1 h_2|$, since for larger $|h_1 h_2|$ the influence of the correction terms $\Delta(h_1,h_2)$ and the choice of 'walking path' (i.e. the signs of h_1 and h_2, resulting in the different 'branches' in the scatterplot) grows. Because $[V,W]_p^{\perp} = 0$ only if sheet structure is present, $E_p^{\perp}(V,W)$ can be used as an indicator of sheet structure. Fig. 4 shows the absolute error of $E_p^{\perp}(V_2,W_2)$ (averaged over 50 noise iterations) as a function of maximum $|h_1 h_2|$ and noise level κ. For higher noise levels, a lower maximum $|h_1 h_2|$ gives the best estimate of $E_p^{\perp}(V_2,W_2)$, as errors accumulate along pathways. Figs. 5 (a) and (b) show $E_p^{\perp}(V,W)$ for pair 1 and 2 as a function of noise and voxel size, respectively. By looking at $E_p^{\perp}(V,W)$, it is possible to distinguish sheet structure from non-sheet structure, except at high noise levels and large voxel size.

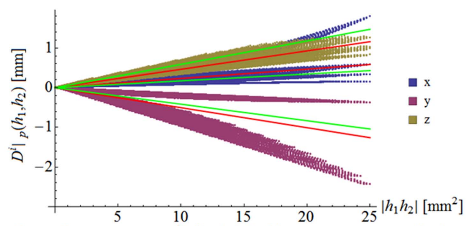

Fig. 3: The components $D^i|_p(h_1,h_2)$ (x: blue, y: magenta, z: yellow) as a function of $|h_1 h_2|$. Red: lines with slope $E^i{}_p(V_2,W_2)$, green: lines with slope $[V_2,W_2]^i{}_p$. $\delta = 0.2\ mm$, $\kappa = \infty$.

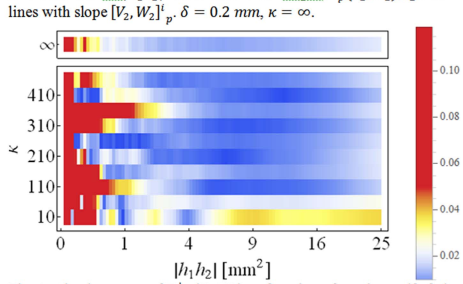

Fig. 4: Absolute error of $E^{\perp}{}_p(V_2,W_2)$ as function of maximum $|h_1 h_2|$ and noise κ (averaged over 50 noise iterations). $\delta = 0.2\ mm$.

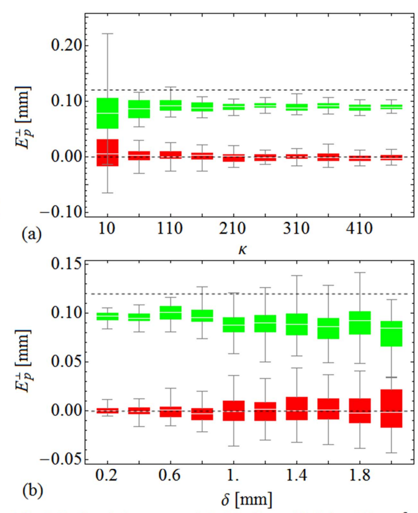

Fig. 5: Red: pair 1, green: pair 2. Maximum $|h_1 h_2| = 25\ mm^2$. Boxplots show the quartiles. (a) $E^{\perp}{}_p(V,W)$ as a function of noise κ with $\delta = 1\ mm$. (b) $E^{\perp}{}_p(V,W)$ as a function of δ with $\kappa = 100$.

Discussion and Conclusion: In this work we have evaluated a method to calculate the discrete Lie bracket for the quantification of sheet structure. By considering the normal component, this approach is indeed capable of differentiating sheets from non-sheet structures being present in these simple vector field examples. Our experiments further show that its performance is dependent on noise level, voxel size, and maximal walking distance along the streamlines. The results will additionally depend on the dMRI reconstruction and tractography method used, and on a number of parameters (e.g. the step size and the stopping criterion), dependencies which we have not considered here. The optimal combination of methods and settings to make this approach as robust as possible, along with quantification of the presence of sheet structure in the brain, are future work.

References: 1. Wedeen et al., Science 335: 1628-1634, 2012; 2. Catani et al., Science 337: 1605, 2012; 3. Wedeen et al., Science 337: 1605, 2012; 4. Spivak, *A comprehensive introduction to differential geometry: Volume I*, Publish or perish, 1999; 5. Misner et al., *Gravitation*, Macmillan, 1973; 6. Wedeen et al., NeuroImage 41: 1267-1277, 2008.